Acta Tropica 158 (2016) 97–106

Contents lists available at ScienceDirect

Acta Tropica

journal homepage: www.elsevier.com/locate/actatropica

In Vitro susceptibilities of wild and drug resistant *Leishmania donovani* amastigotes to piperolactam A loaded hydroxypropyl-β-cyclodextrin nanoparticles

Plaban Bhattacharya[a,b,1], Subhasish Mondal[a,1], Souvik Basak[c], Pradeep Das[d], Achintya Saha[b], Tanmoy Bera[a,*]

[a] Division of Medicinal Biochemistry, Department of Pharmaceutical Technology, Jadavpur University, Kolkata, West Bengal, India
[b] Department of Chemical Technology, University of Calcutta, Kolkata, India
[c] Dr. B.C. Roy College of Pharmacy & Allied Health Sciences, Durgapur, India
[d] Department of Clinical Medicine, Rajendra Memorial Research Institute of Medical Sciences, Indian Council of Medical Research, Agamkuan, Patna, India

ARTICLE INFO

Article history:
Received 24 July 2015
Received in revised form 25 February 2016
Accepted 26 February 2016
Available online 3 March 2016

Keywords:
Piperolactam A
Cylodextrin nanoparticles
Macrophage uptake
Wild-type and drug resistant strains

ABSTRACT

Leishmaniasis is an epidemic in various countries, and the parasite *Leishmania donovani* is developing resistance against available drugs. In the present study the antileishmanial action of piperolactam A (PL), isolated after bioactivity guided fractionation from root extracts of *Piper betle* was accentuated in detail. Activity potentiation was achieved *via* cyclodextrin complexation. Crude hydro-ethanolic extract (PB) and three fractions obtained from PB and fabricated PL-hydroxypropyl-β-cyclodextrin (HPBCD) nanoparticles were evaluated for antileishmanial activity. Tests were performed against *L. donovani* wild-type, sodium stibogluconate, paromomycin and field isolated (GE1) resistant strains in axenic amastigote and amastigote in macrophage models. PL-HPBCD complex was characterized and FITC loaded HPBCD nanoparticles were assessed for macrophage internalization in confocal microscopic studies. Isolated and purified PL from most potent, alkaloid rich ethyl acetate fraction of PB showed high level of antileishmanial activities in wild-type (IC_{50} = 36 μM), sodium stibogluconate resistant (IC_{50} = 103 μM), paromomycin resistant (IC_{50} = 91 μM) and field isolated resistant (IC_{50} = 72 μM) strains together with cytotoxicity (CC_{50} = 900 μM) in mouse peritoneal macrophage cells. Inclusion of PL in HPBCD nanoparticles resulted in 10-fold and 4–10-fold increase in selectivity indexes (CC_{50}/IC_{50}) for wild-type and drug resistant strains, respectively. Drug-carrier interactions were clearly visualized in FT-IR studies. Complete incorporation of PL in HPBCD cavity was ascertained in DSC and XRD analyses. 180 nm size stable nanospheres showed macrophage internalization within 1 h of incubation. Piperolactam A (PL), a representative of the inchoate skeleton of aristolactam chassis might be the source of safe and affordable antileishmanial agents for the cure of deadly *Leishmania* infections.

1. Introduction

Leishmaniasis is a neglected emerging disease, causing severe morbidity and mortality. It has an estimated worldwide incidence of 15 million infected people and 350 million at risk, living in tropical and subtropical areas of 88 endemic countries in America, Europe, Africa, Middle East and Asia (Alvar et al., 2012). The number of deaths as a consequence of leishmaniasis is higher than 50,000 per year (Siqueira-Neto et al., 2010). Causal agents of human leishmaniasis are protozoan parasites that belong to the genus *Leishmania*. They are cycling between (i) blood feeding phlebotomine insects where they develop as extracellular flagellated promastigotes, and (ii) a range of mammals, including rodents, canine hosts and human where they develop as obligatory intracellular amastigotes. Parasite species and the host immune system determines the clinical status of the disease, ranging from cutaneuos ulcers (cutaneuos leishmaniasis) (Reithinger et al., 2007) to visceral organ damage (visceral leishmaniasis) (Chappuis et al., 2007), especially of the spleen and the liver, and is usually fatal if untreated.

Current treatment of leishmaniasis relies on chemotherapy (Singh and Kumar, 2014). No vaccine exists against any form of leishmaniasis and most of the antileishmanial drugs currently in

* Corresponding author.
E-mail address: proftanmoybera@gmail.com (T. Bera).
[1] These authors contributed equally to this work.

http://dx.doi.org/10.1016/j.actatropica.2016.02.017
0001-706X/

use for the treatment, from long time established antimonials to the recently introduced miltefosine, have disadvantages, such as side effects and/or parasite resistance (Croft et al., 2006). Alternative therapeutic approaches based on the use of amphotericin B and its lipid-carrier formulations have been successfully applied when the first line drugs were no longer effective due to drug resistance (Thakur et al., 1996; Gradoni et al., 2008). Nevertheless, very high costs of these drugs prevent their widespread use (Bhattacharjee et al., 2012; Peine et al., 2014). In view of the recent spreading of leishmaniasis due to resistance of first line drugs, there is an urgent need to develop new, safe, fast acting, and affordable treatments (Miguel et al., 2007).

Lead discovery is one of the current trends for searching novel antileishmanial drugs (Nwaka and Hudson, 2006). Wide varieties of secondary metabolites produced in plant species were found to be the source of new potent molecules in several life threatening diseases (Chen et al., 2008; Newman and Cragg, 2012). More than four hundred new botanicals have been processed by Center for Drug Evaluation and Research (CDER) of the U. S. Food and Drug Administration (USFDA), Silver Spring, MD in the last ten years (Lee et al., 2015).

Aristolactam alkaloids, a comparatively untouched class of molecules, were found in several plant species of Piperaceae, Annonaceae, Menispermaceae and Saururaceae families (Marques et al., 2011). Some of those molecules exhibited anti-inflammatory, antiarthritic, anticoagulant activities along with potent antimicrobial action (Odalo et al., 2010; Yang et al., 2010; Levrier et al., 2013). Structurally similar aporphine alkaloids were reported to possess strong antileishmanial potencies and were evaluated only against wild-type strains of *Leishmania* (Waechter et al., 1999; Montenegro et al., 2003; Correa et al., 2006; Silva et al., 2012). Revelation of potent antimicrobial activity of aristolactams along with reported antileishmanial activity of structurally similar aporphines encouraged us to evaluate of antileishmanial activity of aristolactams.

Roots of *Piper betle* have extensively been used in traditional herbal preparations in India, China, Taiwan, Thailand and many other countries (Ali et al., 2010) and known to contain different bioactive secondary metabolites such as ursolic acid, diosgenin, β-sitosterol, stigmasterol, resorcinol along with aristolactams (Lin et al., 2013). Leaves of this plant have been previously reported for potent leishmanicidal action and the volatile oil constituents were hypothecated as the active constituents (Sarkar et al., 2008; Misra et al., 2009). In our experiment, a targeted approach towards isolation of aristolactams from roots of *P. betle* has been carried out. As the isolated molecule piperolactam A (PL) exhibited promising leishmanicidal action against wild type strains of *Leishmania donovani in vitro*, in comparison to standards and aporphines (Waechter et al., 1999; Montenegro et al., 2003; Correa et al., 2006; Silva et al., 2012), we have chosen PL for further investigation. PL was evaluated for *in vitro* antileishmanial activity against sodium stibogluconate (SSG), paromomycin (PMM) and field isolated (GE1) resistant strains in axenic amastigote and amastigote in macrophage models.

Formulation development is an integral part of all drug discovery processes. In our formulation, cyclodextrin was used as solubility enhancer, stabilizer, taste masking agent and also sustained release carrier. Diverse types of compounds are generally entrapped in cyclodextrin cavities and the inclusion complexes served as deft delivery device for exhibition of potent action. The hydroxypropyl derivative of β-cyclodextrin *i.e.*, 2-hydroxypropyl-β-cyclodextrin (HPBCD) has advantage for its better complexation ability and lesser toxicity than that of natural cyclodextrins (Stella and He, 2008). Morever, HPBCD has been already established as a antileishmanial drug carrier (Pucadyil et al., 2004; Demicheli et al., 2004). In the present study, PL-HPBCD inclusion complex was prepared for enhanced bioavailability and to overcome multidrug resistance.

2. Materials and methods

2.1. Ethics statements

BALB/c mice of either sex, weighing between 20 and 25 g were used for the study. The experimental protocols were approved by the Jadavpur University Animal Ethics Committee, and procedures followed were in accordance with the Committee's guidelines, with necessary humane care. Mice were housed in polypropylene cages and fed with standard diet and water ad libitum. Animals were exposed to normal day and night cycle.

Roots of *P. betle* Linn., Piperaceae (Kali Bangla variety) were collected from Tamluk, eastern Medinipur district of West Bengal, India and authenticated by the Central National Herbarium, Botanical Survey of India (voucher no.-CNH/I-I/276/2008/Tech.II/318). The plantation was carried out on private land. The owner of the land gave us prior permission to conduct the study. Our study did not involve any endangered or protected species. People of West Bengal generally are habituated to use the leaves of this plant to chew for digestive purpose. The leaves are readily available in markets.

2.2. Extract preparation, bioactivity guided fractionation and isolation

Cleaned roots were shade dried and subsequently powdered. Powdered material was extracted with 70% ethanol (1:8 w/v, solvent polarity index = 6.34) by continuous hot percolation in soxhlet extractor for 6 h. One portion of the extract solution was concentrated under vacuum and successively extracted with *n*-hexane and ethyl acetate. Antileishmanial activity was screened with the crude hydro-ethanolic extract along with three fractions *i.e.*, *n*-hexane, ethyl acetate and the last remnant. Phytochemical analyses were performed for assessment of the presence of the class of phytochemical moieties (Harborne, 1998).

The ethyl acetate fraction was found to be most potent and exhibited prominent presence of alkaloids in Mayer's and Dragendorff's test (Harborne, 1998). The ethyl acetate fraction (Yield ~120 g) was subjected to column chromatography on silica gel (60–120 mesh). Column was eluted with a gradient of hexane/ethyl acetate (95:5–0:100). The hexane:ethyl acetate (50:50) fraction showed most prominent presence of alkaloids and was subjected to further purification by preparative TLC over silica gel (0.3 mm thickness) plate prepared in CAMAG TLC plate coater (Bhattacharya and Saha, 2013). Toluene-ethyl acetate-methanol mixture (3:2:1) was used as mobile phase. After development of chromatogram, the separated line stretches were visualized by UV light and the major component showing intense fluorescent band at 366 nm removed and recovered by treating the adsorbent with methanol. The yellow solid precipitate was recrystallised from ethanol (yield: 108 mg) and identified by melting point, HPTLC, UV, FT-IR, NMR and MS spectroscopic studies.

2.3. Preparation of PL-HPBCD inclusion complex

The isolated compound piperolactam A, (PL) was found to be poorly water soluble and to enhance the solubility and bioavailability, inclusion complex was prepared with 2-hydroxypropyl-β-cyclodextrin (HPBCD) (Memisoglu et al., 2003). Aqueous solution of HPBCD (0.5 mM) was mixed with PL in 70% ethanol (1:1 molar ratio). The mixture was placed over a magnetic stirrer for 12 h followed by centrifugation for removal of unentrapped drug. The supernatant was filtered through 0.45 μm filter.

Excess solvent, mainly ethanol was removed from the complex using rotary evaporator at 70 °C and ultra-centrifuged. The precipitates were lyophilized and stored in a desiccator at 4 °C. Powders were dispersed in distilled water prior to administration. Content of PL in developed PL-HPBCD complex was assessed by HPTLC (linearity range 100–400 ng, $r^2 > 0.99$) with solvent system comprising of toluene-ethyl acetae-methanol (3:2:1) (Bhattacharya et al., 2014). FITC loaded HPBCD nanoparticles were also prepared as depicted above.

2.4. Characterization of PL-HPBCD inclusion complex

2.4.1. Transmission electron microscopy

The morphology of nanoparticles was examined by the conventional negative staining method with FEI Tecnai TM Transmission Electron Microscopy (Netherland) which was operated with an acceleration voltage of 80 kV. One drop of nanoparticle was placed over the carbon-coated copper grids and then these grids were washed with distilled water. Then staining was performed with uranil acetate solution. Sample was air-dried before observation.

2.4.2. Dynamic light scattering (DLS) study

Size distribution of PL-HPBCD inclusion complex were assessed in triplicate by Zetasizer Nano ZS (Malvern, UK) at a concentration of 1 mg/mL in HPLC grade water. Zeta potential (mV) was measured for estimation of surface charge and the stability of the system.

2.4.3. FTIR studies

The FTIR studies were carried out to observe the probable drug-carrier (PL-HPBCD) interactions in the inclusion complex. Samples (PL, HPBCD and PL-HPBCD complex) were triturated separately with IR grade KBr in the ratio of 1:100 and were pelletized in a hydraulic press. The pellets were scanned over a wavenumber range of 4000–400 cm^{-1}.

2.4.4. Differential scanning calorimetric (DSC) analysis

DSC experiments were conducted in a Mettler TA4000 differential scanning calorimeter under constant flow of nitrogen gas. Samples were sealed in crimped aluminum pans and heated at the speed of 10 °C/min from 0 to 350 °C.

2.4.5. X-ray diffraction (XRD) analysis

XRD of isolated molecule PL, HPBCD and PL-HPBCD were recorded with a XPERT-PRO X-ray diffractometer (Model: PW 3050/60, PANalytical, Almelo, Netherlands). The 2θ range is 5–60 ° and the scan rate is 1°/min with Cu $K\alpha$ radiation (40 kV, 30 mA).

2.4.6. In vitro *release kinetics*

Release kinetics of PL from PL-HPBCD nanospheres were determined after incubation (37 °C) in phosphate buffered saline (PBS) pH 7.4 providing sink conditions in a thermostated shaker bath system. At given time intervals, 2 mL samples were withdrawn from the system and replaced with equal volume of fresh release medium (Memisoglu et al., 2003). Samples were centrifuged and the PL content was assessed by developed HPTLC method as described earlier (Bhattacharya et al., 2014).

2.5. Parasites and culture conditions

Promastigotes of *L. donovani* clones, AG83 (MHOM/IN/83/AG83) and GE1 (MHOM/IN/80/GE1F8R) were VL isolates obtained as a gift from Indian Institute of Chemical Biology, Council of Scientific and Industrial Research, Kolkata, India. Antimony-sensitive strain, AG83 and antimony-resistant isolate, GE1 were characterized earlier (Mookerjee et al., 2008; Biyani et al., 2011). AG83 is generally used to consider as reference standard strain of *L. donovani* in India. Parasites were routinely grown as promastigotes in medium 199 supplemented with 10% heat—inactivated fetal calf serum (FCS) at 24 °C.

2.6. Resistance selection to sodium stibogluconate and paromomycin on promastigotes and their transformation to drug resistant amastigotes

The wild-type AG83 promastigote cells were cultured in medium 199 (with supplements), in the presence of drug concentration corresponding to the 50% inhibitory concentration (IC_{50} values of SSG and PMM were 3.6 μg/mL and 10 μM, respectively) of the strain. Sodium stibogluconate and paromomycin resistant phenotype clones were designated as AG83-R. The procedure was performed according to the previous published work (Iovannisci and Ullman, 1983; Kar et al., 1990; Mondal et al., 2013).

2.7. Generation of axenic amastigotes

L. donovani amastigote forms were grown and maintained as described by Debrabant et al., 2004. Axenically grown amastigotes of *L. donovani* were maintained at 37 °C in 5% CO_2/air by weekly sub-passages in MMA/20 at pH 5.5 in petri dishes (Teixeira et al., 2002) as described previously (Mondal et al., 2013; Roy et al., 2010).

2.8. Cross-resistance and sensitivity studies

Cross-resistances of sodium stibogluconate (SSG) resistant AG83 to paromomycin (380 μM) (PMM), and paromomycin resistant AG83 to sodium stibogluconate (115 μg/mL) were determined by measuring 50% inhibitory concentration (IC_{50}) by cell counting method using hemocytometer. Similarly, sensitivity (IC_{50}) of SSG to SSG resistant AG83 (130 μg/mL), sensitivity of PMM to PMM resistant AG83 (360 μM) and IC_{50}s of SSG (11 μg/mL) and PMM (23 μM) to GE1 strain were determined by cell counting. To measure the IC_{50} values, the parasites were seeded into 96-well plates at a density of 1 × 104 promastigotes/well or 1 × 105 amastigotes/well in 200 μL medium containing 10 μL of different drugs. Parasite concentrations in treated plates were compared to that of untreated control (100% growth). After 72 h of incubation, cell counts were taken microscopically. The results were expressed as the percentage of reduction in parasite number compared to that of untreated control wells, and the IC_{50} values were calculated by linear regression analysis (MINITAB V.13.1, PA) or linear interpolation (Huber and Koella, 1993).

2.9. Amastigotes in macrophage drug susceptibility assay

The method was performed according to the previous published work (Mondal et al., 2013). Briefly, macrophages were isolated from the peritoneal lavage of BALB/c mice. A suspension of 4 × 106 amastigotes in RPMI-1640 was added in a 500 μL volume to each well (macrophage/parasite ratio of 1:10). The plates were incubated for 4 h at 37 °C in 5% CO_2 and the medium was aspirated to remove free parasites. Fresh 1 mL RPMI-1640 with or without drugs or nanoparticles at the appropriate concentration was added in triplicate wells. Plates were incubated for 72 h at 37 °C in 5% CO_2. The medium was aspirated and the cover slips were removed and then methanol fixed and air dried. After staining with Giemsa, 100 cells on the glass disks were counted. Three independent experiments in triplicate for each concentration were performed for efficacy of drugs or nanoparticles. Results were presented as the ratio between the infection proportions of treated and untreated macrophage cultures.

Table 1
Evaluation of sensitivity profile of extracted fractions from *Piper betle* against *Leishmania donovani* AG83 wild-type axenic and intracellular amastigote cell lines.

Extract/fractions	IC_{50} (mean ± SD, n = 3) μg/mL[a]	
	Axenic evaluation model	Cellular evaluation model
Hydro-ethanolic	93 ± 12	84 ± 10
n-Hexane	124 ± 25	109 ± 18
Ethyl acetate	22 ± 3.18	14 ± 2.52
Last remnant	Inactive	Inactive

[a] Assays are described in Section 2.

2.10. Nanoparticle cellular uptake

In order to study nanoparticle uptake in macrophage cells, the desired cell concentration (4 × 105 cells/well) was seeded with fluorescent FIT C-HPBCD nanoparticles (0.5 mg/mL), and incubated in CO_2 incubator at 37 °C for 15, 30 and 60 min time intervals. Samples were observed in FITC channel under fluorescence microscope (magnification 60×).

2.11. Cytotoxicity assay and selectivity index

Macrophages cells were cultured in RPMI-1640 medium supplemented with 10% FCS, 20 mM L-glutamine, 16 mM $NaHCO_3$, penicillin (50 U/mL) and streptomycin (50 μg/ mL). The assay was performed in 96-well tissue culture plates in the presence of 2×10^5 macrophages. The wells were seeded with test solutions and the viable macrophages were counted microscopically. The selectivity index (SI) which is typically considered as the highest exposure to the drug that results in no toxicity to that exposure that produces desired efficacy—is an important parameter in efforts to achieve this balance. In the present study, the degree of selectivity of the drug or its formulation is expressed as $SI = CC_{50}$ of a drug or its formulation in a macrophage cell line/IC_{50} of the same drug or its formulation, where CC_{50} is the concentration required to kill 50% of the host cell population and IC_{50} is the concentration required to kill 50% of the parasites inside the host cell. When the SI value is ≥10, that drug or formulation presents promising activity, that is higher than its cytotoxicity (Nwaka and Hudson, 2006).

2.12. Statistical analysis

Experimental results were expressed as mean ± standard deviation. Student's *t*-test was used to calculate the statistical difference of mean values. Differences were considered significant at a level when $p < 0.05$.

3. Results

3.1. Characterization of isolated compound

Qualitative chemical examinations of *P. betle* root extract exhibited prominent presence of steroids, terpenes, alkaloids and saponins. An aristolactam alkaloid was isolated from the most potent ethyl acetate fraction (Table 1, Fig. 1) and characterized as piperolactam A (Fig. 2). The characteristics were analyzed as follows: yellow needles; melting point >300 °C; UV (MeOH) λ_{max} 235, 264, 278, 287, 318, 385 nm; single spot and intense fluorescence at 366 nm at R_f values of 0.62 ± 0.08 (n = 4), in solvent systems comprising of toluene-ethyl acetate-methanol in the ratios of 3:2:1; no other peak was detected after charring with freshly prepared 10% methanolic sulphuric acid; IR (KBr) ν_{max} 3471, 3177 (broad peaks of OH stretching), 1656 (C=O stretching) and 1616 (NH bending) cm^{-1}; ^1H NMR (300 MHz, DMSO-*d*6) δ 4.04 (3H, s, 3-OCH_3), 7.12 (1H, s, H-9), 7.54 (2H, m, H-6, H-7), 7.76 (1H, s, H-2), 7.92 (1H, m, H-8), 9.25 (1H, m, H-5), 10.62 (1H, br s, D_2O exchangeable, N—H) (Fig. 2A); ^{13}C NMR (125 MHz, DMSO-*d*6) δ 57.4 (3-OCH_3), 105.8 (C-9), 110.6 (C-2), 114.4 (C-4a), 115.6 (C-1), 124.1 (C-11), 124.8 (C-7), 125.9 (C-6), 126.1 (C-8a), 126.9 (C-5), 127.6 (C-8), 133.8 (C-5a), 134.8 (C-10), 148.7 (C-4), 149.9 (C-3), 168.8 (C-12) (Fig. 2B); HREIMS *m/z* 265.1074 (Fig. 2C). The position of methoxy group in the phenanthrene nucleus was confirmed from the HMBC spectrum, in which the corresponding proton signal (δ 4.04) was correlated with C-3 (δ 149.9) (Lin et al., 2013; Lo et al., 2000; Desai et al., 1988).

3.2. Characterization of PL-HPBCD complex

TEM image clearly depicted the spherical shape and morphology of the developed PL-HPBCD complex (Fig. 3). The average hydrodynamic particle diameter was found to be 180.4 ± 16.42 nm with a poly-dispersity index of 0.232 in DLS study along with zeta potential of −28.6 ± 1.54 mV. Content of PL in developed PL-HPBCD complex was assessed by HPTLC method described in Section 2.3 and the final molar ratio between PL to HPBCD was found to be 0.45 ± 0.02 (n = 3).

The FT-IR spectrum showed interaction pattern of PL with HPBCD in the developed formulation (Fig. 4A). The peaks of PL and HPBCD were overlapped in the region of 2500–3800 cm^{-1}. The peak of PL at 1616 cm^{-1} was shifted to 1610 cm^{-1} due to hydrogen bond formation between the secondary amine (NH) and hydroxyl group of cyclodextrin molecules. The carbonyl stretching in 1656 cm^{-1} was found to be shifted to 1689 cm^{-1}, which probably indicates the disappearance of inter-molecular interactions of carbonyl and secondary amines and suggests incorporation of piperolactam in cyclodextrin cavity as monomer (Carrizosa et al., 2004). The stretching vibration of PL at 1452 cm^{-1} (phenanthrene nucleus) was found to be greatly diminished in developed PL-HPBCD complex, due to inclusion of major portions of phenanthrene ring in cyclodextrin cavity.

Fig. 4B shows the DSC curves of PL, HPBCD and PL-HPBCD complex. The DSC curve of piperolactam A showed an endothermic peak at about 310.12 °C corresponds to its melting point. The DSC curve of the complex mainly showed the pattern of HPBCD, in which the characteristic endothermic peaks of PL was disappeared. It was considered that PL had been completely incorporated in HPBCD cavity and they should have some interaction, such as the combination of hydrogen bonds and/or van der Waals force.

The interaction of drug (PL) with HPBCD was clearly visible in XRD patterns (Fig. 4C). In the product, the crystallographic peaks of the isolated molecule were fully abolished and the XRD pattern of PL-HPBCD was found to be merely super-imposable with solitary HPBCD. These indicate formation of amorphous state, complete dilution in the carrier cavity and complexation. Demolition in crystalline nature obviously pretends a role for better oral bioavailability.

The major drawback of various designed inclusion complexes from cyclodextrins is the initial burst release of drug. This is partly overcome in this experimental work mainly after size reduction (Memisoglu et al., 2003). Only 60% cumulative release after 1 h clearly directed incorporation of PL in HPBCD cavity (Fig. 5). It might be due to incorporation of ethanol during 12 h complexation process. Dissolution of PL from developed nano inclusion complex formulation was probably due to replacement of PL from cyclodextrin cavity by buffer components and makes the formulation suitable for oral, i.v. as well as topical delivery.

3.3. SSG and PMM resistance selections in promastigotes

Selection process by stepwise drug pressure for AG83-R phenotype was found to be limiting at 34 μg Sb(V)/mL for SSG and

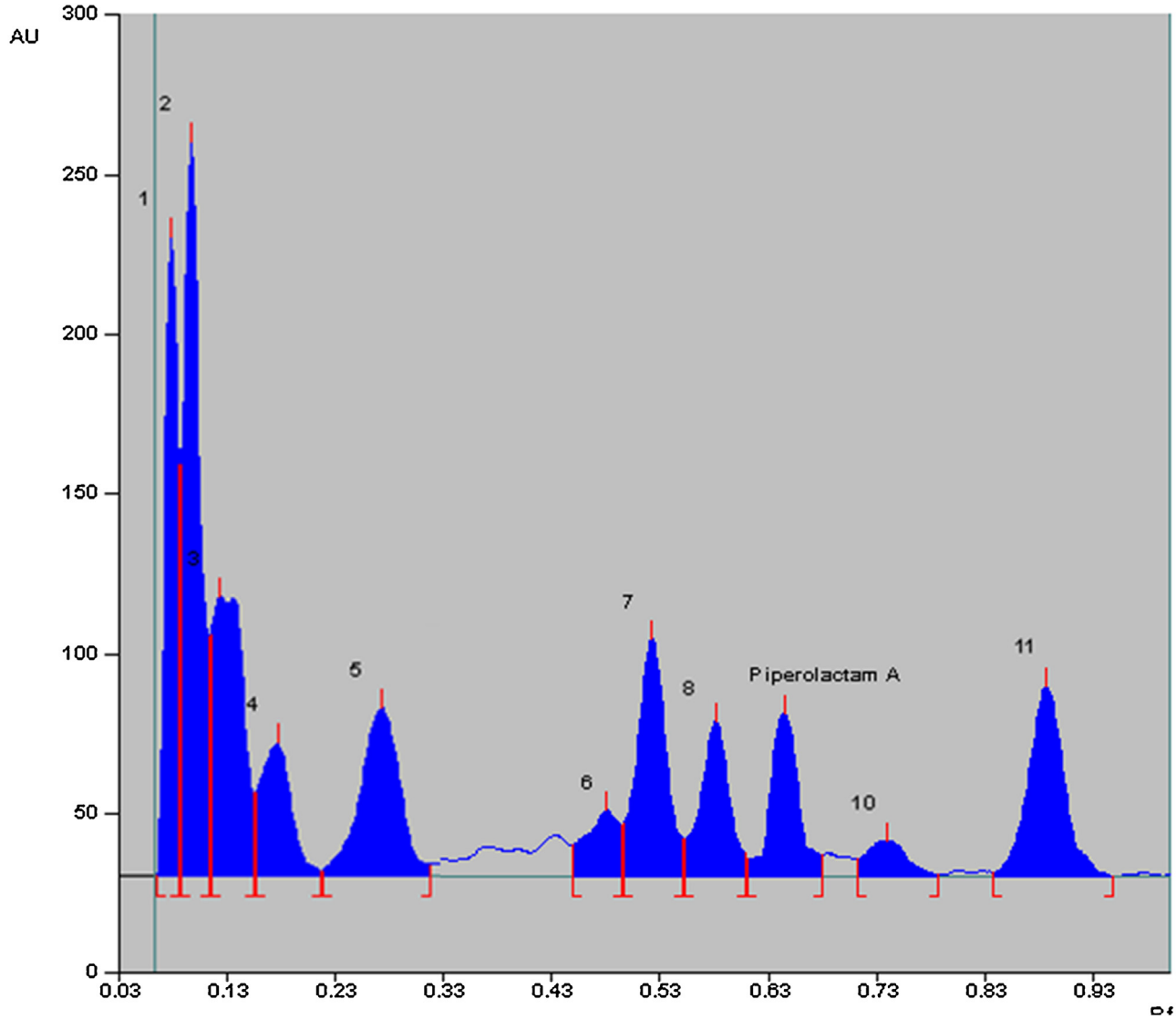

Fig. 1. HPTLC chromatogram of ethyl acetate fraction of hydro-ethanolic extract of *Piper betle* root. Stationary phase was TLC Silica Gel G, Solvent system comprising of toluene, ethyl acetate and methanol (3:2:1), densitometric scanning was performed at absorbance-reflectance mode at 366 nm of wavelength in TLC scanner 3 with WINCATS software version 1.4.2. Distinct peak of PL at R_f of 0.65.

Table 2
Drug sensitivity profiles against *Leishmania donovani* wild-type, drug resistant and field isolated axenic amastigote cell lines.

Drug	IC_{50} (mean ± SD, n = 4) μM[a]						
	Axenic AG83 evaluation model					Axenic GE1 evaluation model	
	Wild-type	SSG resistant[b]	RI[c]	PMM resistant[b]	RI[c]	Field isolate	RI[d]
Amphotericin B	0.2*	0.21 ± 0.05*	1.0	0.23 ± 0.05*	1.1	0.2 ± 0.05*	1
SSG (SbV)[e]	3.6 ± 0.40	130 ± 20	36	115 ± 16	32	11 ± 1.8	3
PMM	10 ± 2*	380 ± 40*	38	330 ± 30*	33	23 ± 3.6**	2
Miltefosine	0.42 ± 0.048*	0.64 ± 0.056*	1.5	0.54 ± 0.12*	1.3	0.50 ± 0.15*	1.2
Piperolactam A (PL)	60 ± 9.6*	121 ± 18**	2	109 ± 15***	1.8	87 ± 12*	1.5
Nanopiperolactam A (PL-HPBCD)	18 ± 2.4*	40 ± 6*	2.2	33 ± 4.8*	1.8	25.2 ± 4.2**	1.4

[a] Assays are described in Section 2.
[b] SSG and PMM resistant strains were generated *in vitro* as given in Section 2.
[c] RI, Resistance Index was defined as IC_{50} of AG83 phenotype generated at maximum drug pressure/IC_{50} of wild-type.
[d] RI, Resistance Index was defined as IC_{50} of field isolate/IC_{50} of wild-type.
[e] Values for antimonial agents were in μg Sb/mL.
** $p < 0.5$, no significant difference compared with SSG.
*** $p > 0.5$, no significant difference compared with SSG.

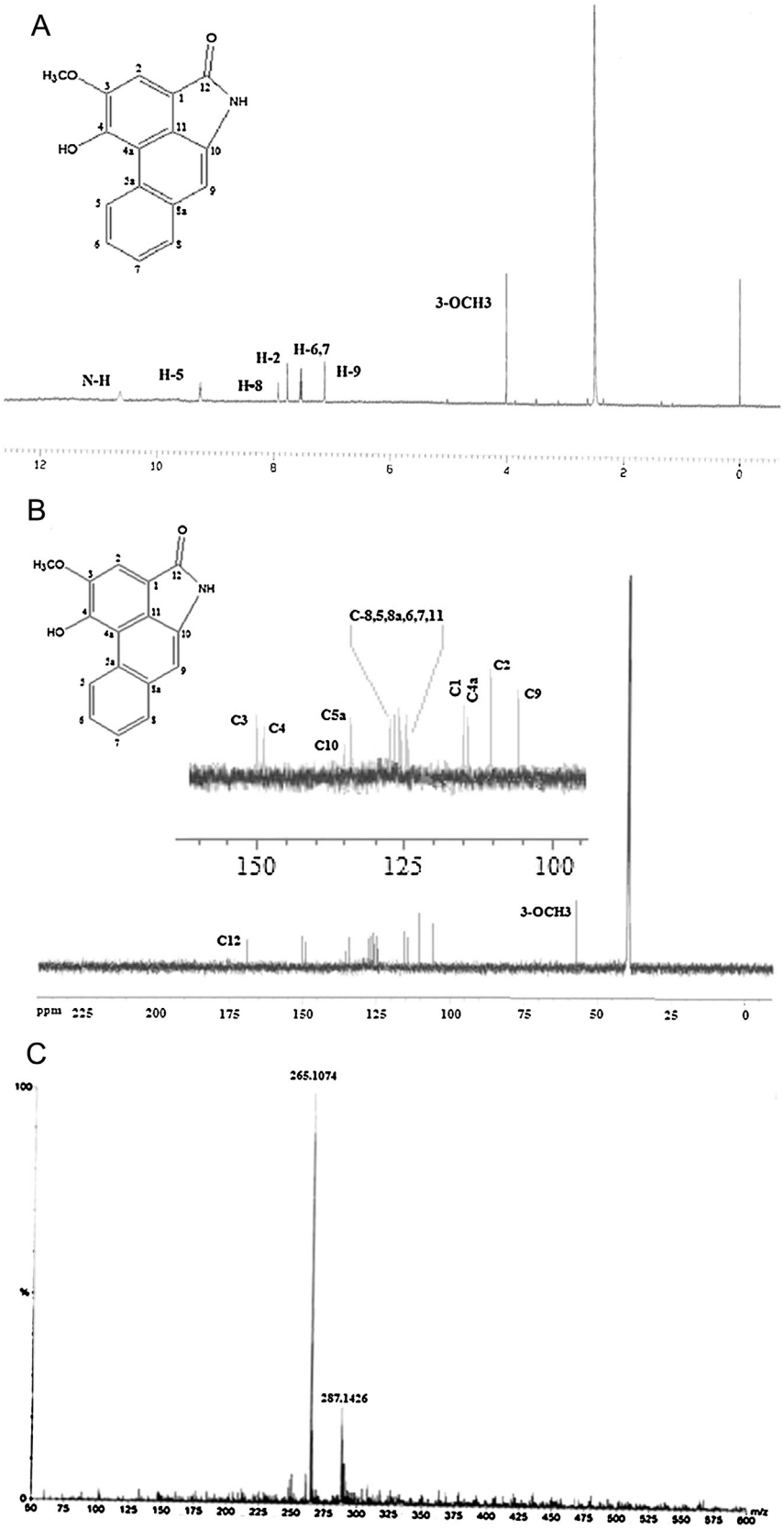

Fig. 2. NMR and Mass-spectral analyses for structural elucidation of purified aristolactam alkaloid obtained from ethyl acetate fraction from *Piper betle* root. (A) ^{1}H NMR, 300 MHz, DMSO-*d*6; (B) ^{13}C NMR, 125 MHz, DMSO-*d*6; and (C) mass spectrum ([M]+ *m*/*z* 265.1074).

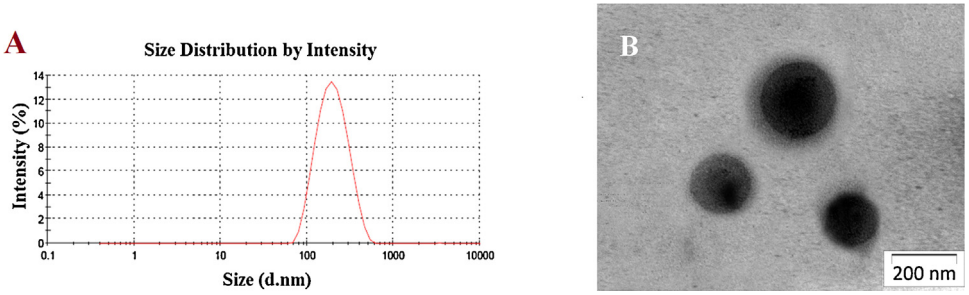

Fig. 3. (A) particle size distribution by DLS study. PL-HPBCD inclusion complex showed a near perfect Gaussian size distribution. (B) Visualization of particle shape and size of PL-HPBCD nanoparticles by TEM (magnification 30,000×, acceleration voltage: 80 kV). One drop of nanoparticle was placed over the carbon-coated copper grids. Sample loaded copper grids were washed with distilled water. Then staining was performed with uranil acetate solution and sample was air-dried before observation.

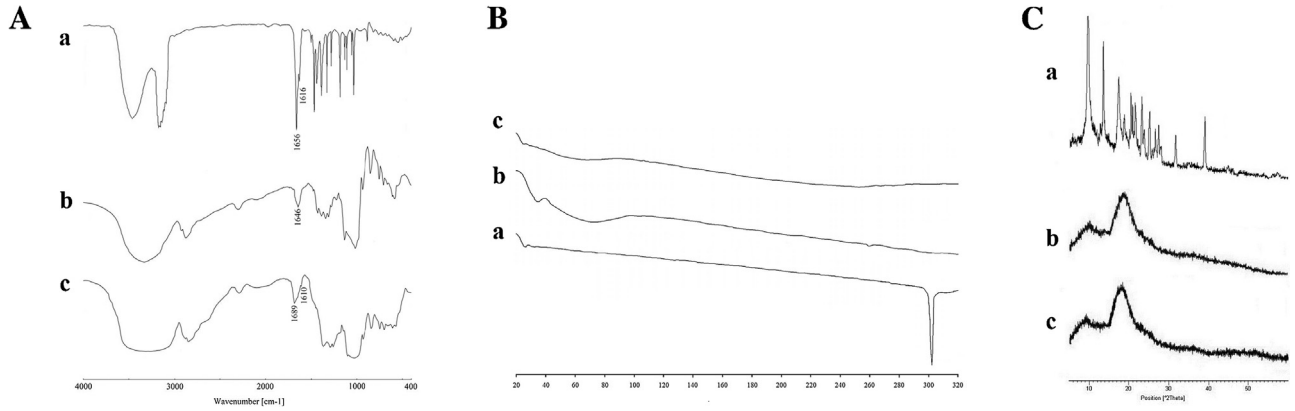

Fig. 4. Characterization of piperolactam A (PL) loaded HPBCD nanoparticles. (A) FT-IR spectroscopic studies depicted drug-carrier interactions, hydrogen bond formation between secondary amino group of PL with hydroxyl groups of cyclodextrins (B) differential scanning calorimetric (DSC) thermograms ascertained complete dilution of PL in cyclodextrin cavity and (C) XRD characteristics depicted abolition of crystallinity of PL in PL-HPBCD. (a) PL crystal, (b) HPBCD and (c) PL-HPBCD complex.

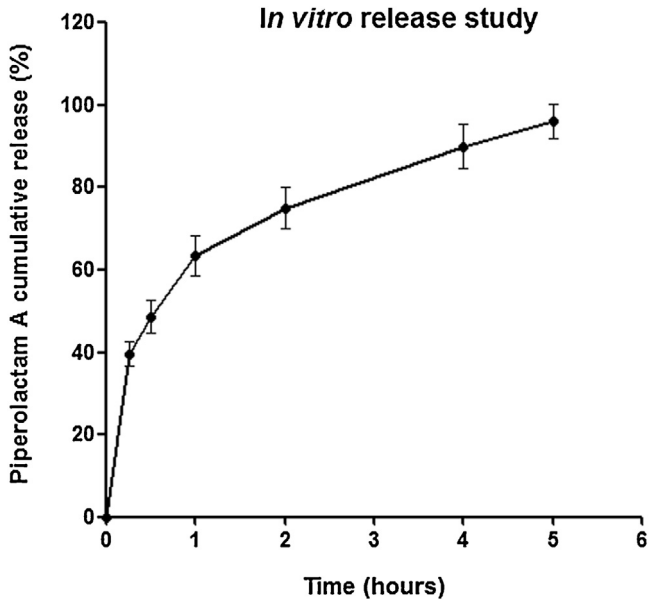

Fig. 5. Piperolactam A release profile in isotonic phosphate buffer. Results expressed as mean ± S.D. (n = 3). The time dependent *in vitro* release of PL was studied and the average percentage cumulative release over time was plotted.

165 μM for PMM when 90% of total cell population was subjected to death in comparison to untreated cells (Mondal et al., 2013). When growth rates of finally selected cell lines (AG83-R) proved to be fully comparable to that of the parent non-selected strains, promastigotes were transformed to amastigotes. The comparison of IC_{50} values between the parent and the resistance-selected phenotypes revealed large differences. AG83-R showed a 32–38-fold increase in IC_{50} for PMM and SSG when compared with wild-type as shown by RI values in Table 2. Field isolate GE1 showed three-fold SSG resistance and two-fold PMM resistance (Table 2). Resistance index (RI) values of amphotericin B for AG83-R and GE1 were found to be 1, which suggested that amphotericin B was equally effective for wild-type, drug resistant and field isolated strains. RI values of miltefosine for AG83-R and GE1 strains remained within the range of 1.2–1.5, suggesting that miltefosine was effective for AG83-R and GE1 strains and may be considered second to amphotericin B in their ranking. Strikingly, miltefosine and piperolactam A showed very low (1.2–2) resistance indexes for AG83-R and GE1 strains. Resistance indexes for nanopiperolactam (PL-HPBCD) ranged from 1.4 to 2.2 for AG83-R and GE1 strains, little higher than free piperolactam. Thus, free PL and PL-HPBCD appeared to be potentially potent to inhibit the cell growth of AG83-R and GE1 amastigotes.

3.4. In vitro *susceptibilities of nanopiperolactam a (PL-HPBCD) on AG83 wild-type, AG83-and GE1 cellular amastigotes*

It appeared from the cellular evaluation model (Table 3) that both amphotericin B and miltefosine showed very high selectivity indexes (SIs) for wild-type, AG83-R and GE1 strains. SIs of SSG and PMM were dramatically reduced in AG83-R strains, whereas GE1 strain showed SI values intermediate between AG83-R and wild-type strains. SIs of piperolactam A in wild-type and GE1 strains were very similar to each other. Strikingly enough, when piperolactam A was formulated as nanopiperolactam A (PL-HPBCD, particle size 180 nm), SI values in wild-type and GE1 strains increased compared to free piperolactam A, 10-fold and 5-fold, respectively. However,

Table 3
Drug sensitivity profiles of intracellular amastigotes against wild-type, drug resistant and field isolated *Leishmania donovani* cell lines.

Drug	IC_{50} (mean ± SD for at least 4 replicates) μM [a]								
	Cellular AG83 evaluation model						Cellular GE1 evaluation model		
	Wild-type	SI[d]	SSG resistant[b]	SI[d]	PMM resistant[b]	SI[d]	Field isolate	SI[d]	Cytotoxicity CC_{50} (μM) (Macrophage cells)
Amphotericin B	0.15 ± 0.0*	93	0.2 ± 0.05*	70	0.20 ± 0.05*	68	0.16 ± 0.05*	87.5	14 ± 2.1**
SSG (SbV)[c]	1.6	17	18.1 ± 3	1.5	17.3 ± 2.60	1.6	7.7 ± 0.65	3.5	27 ± 3.9
PMM	8 ± 2*	31	125 ± 15*	2	115 ± 13*	2.1	18 ± 3*	13.8	248 ± 32*
Miltefosine	0.36 ± 0.06*	96	0.60 ± 0.15*	57.5	0.46 ± 0.0.8*	75	0.39 ± 0.12*	88	34.5 ± 6.3**
Piperolactam A	36 ± 4.8*	25	103 ± 12*	8.7	91 ± 20*	9.9	72 ± 10*	12.5	900 ± 120*
Nanopiperolactam A (PLHPBCD)	4.84 ± 0.6*	248	36 ± 6.2**	33.3	24.5 ± 4.5**	49	18 ± 3.3*	66.6	1400 ± 200*

[a] Assays are described in Section 2.
[b] SSG and PMM resistant strains were generated *in vitro* as given in Section 2.
[c] Values for antimonial agents are in μg Sb/mL
[d] SI, Selectivity Index was CC_{50}/IC_{50}.
* $p < 0.001$, significant difference compared with SSG.
** $p < 0.5$, no significant difference compared with SSG.

SI values of nanopiperolactam A in AG83-R strains increased compared to free piperolactam A, 4-fold for SSG resistant strain and 5-fold for PMM resistant strain. Since, SI values of nanopiperolactam A in wild-type, AG83-R and GE1 strains were greater than 10, we may expect that nanopiperolactam A would be therapeutically safe for intervention of infections with wild-type and GE1 strains. Moreover, we had tested the effect of HPBCD itself on both amastigote and amastigote in macrophage models. However, results showed that multiplication of amastigotes remained unaffected by HPBCD even at a concentration >1000 μM.

3.5. Nanoparticle cellular uptake

A separate set of experiments with FITC-loaded HPBCD nanoparticles was carried out to study the cellular uptake in peritoneal macrophage cells at different time intervals. The prepared nanoparticles showed considerable increase in cellular internalization within 1 h of incubation when compared with 15 min (Fig. 6). The figure represented time dependent uptake of FITC-loaded HPBCD nanoparticles.

4. Discussion

Sodium stibogluconate (SSG) is the drug of choice against *Leishmania* infection and resistance to this drug is a major problem (Rojas et al., 2006; Sundar et al., 2000; Lira et al., 1999; Faraut-Gambarelli et al., 1997; Jackson et al., 1990). Chemotherapeutic alternatives like paromomycin and miltefosine are susceptible for development of drug resistant strains (Jhingran et al., 2009; Perez-Victoria et al., 2003). Unfavorable aqueous solubility profile of investigated compounds is also an important factor for the chemotherapeutic agent to be effective. About half of the potentially valuable drug candidates identified by high throughput screening demonstrated poor aqueous solubility. For this reason drugs were not developed further, and failed to enter formulation development pipe lines.

Plant extracts, as a natural blend of phytochemicals, offer immense opportunities for discovery of active constituents, an archetype of current pharmaceutical industries (Rasoanaivo et al., 2011). Fractionation using classical chromatography has been widely used for isolation of active ingredients from plant extracts (Sasidharan et al., 2011; Dinan et al., 2001). On similar lines of thought, we had extracted root of *P. betle* with hydro-alcoholic mixture followed by fractionation. Presence of alkaloid was found to be most prominent in the most active (Table 1) ethyl acetate fraction. An aristolactam alkaloid was isolated from this ethyl acetate fraction and characterized as piperolactam A (PL) (Fig. 2A–C). PL, a promising alternative antileishmanial agent (Table 2), is marred by solubility and bio-distribution limitations. Our group has studied to enhance solubility and cellular uptake of PL by complexing with 2-hydroxypropyl-β-cyclodextrin (HPBCD) as inclusion complex which is presented in this research work. FT-IR spectroscopic studies clearly depicted drug-carrier interaction (Fig. 4A). Hydrogen bonds were formed between the secondary amino group of PL and hydroxyl groups of cyclodextrin. The crystalline nature of PL was found to be demolished in PL-HPBCD inclusion complex (Fig. 4C) and complete molecular entrapment of PL in cyclodextrin cavity further confirmed inclusion complex formation (Fig. 4B).

We observed that SSG and PMM resistant cell lines of AG83-R were 32–38-fold more resistant than wild-type AG83, whereas field isolate GE1 strain was only 2–3 fold more resistant (Table 2, $p < 0.05$). In contrast, amphotericin B, miltefosine and PL were equipotent to wild-type AG83, AG83-R and GE1 strains. Inclusion of PL in HPBCD as nanopiperolactam A did not alter the RI values significantly (Table 2). If we consider SI values, nanopiperolactam revealed maximum selectivity among amphotericin B, SSG, PMM, miltefosine and free PL for wild-type AG83 (Table 3). Nanopiperolactam A revealed 2.6-fold higher selectivity than second-line drug of choice amphotericin B and miltefosine for wild-type AG83 strain. However, nanopiperolactam A was similar in SI to amphotericin B and miltefosine for field isolate GE1 strain. From these observations, we may conclude that nanopiperolactam A was able to overcome drug resistance. Inclusion of paclitaxol in HPBCD showed similar results in MDR breast cancer cells (Baek and Cho, 2013). The toxic nature of developed PL-HPBCD nanoparticles towards *Leishmania* amastigotes were visualized by TEM studies. Major observations related to structural alterations of leishmanial cells were deformated cellular membrane, formation of massive cytoplasmic vacuolization and mitochondrial swelling indicating cellular toxicity after 4 h of incubation. Aristolactams are generally nephrotoxic. PL-HPBCD had failed to produce progressive kidney damage after 14 days of oral administration as judged from ^{1}H NMR studies of D_2O extracts of rat kidney by super-imposable PCA scores (Suppl. Fig. 1, Suppl. Table 1).

Amastigotes are the mammalian infective forms which reside inside the phagolysosome of macrophages responsible for pathogenesis, whereas promastigotes are the infective forms in sandfly vector. There are remarkable differences between these two forms with respect to biochemical and mitochondrial bioenergetics functions (Chakraborty et al., 2010; Mondal et al., 2014a,b). Most of the active antileishmanial compounds tested on promastigotes failed to inhibit amastigotes (Mattock and Peters, 1975; Peters et al.,

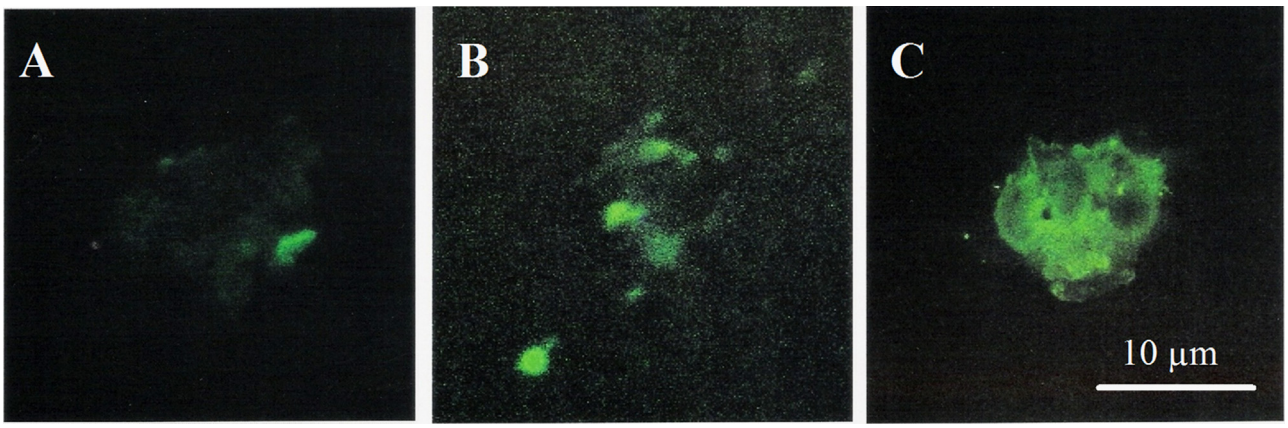

Fig. 6. Time-dependant uptake of PL-HPBCD nanospheres in peritoneal mice macrophages. Fluorescence image. FITC-loaded HPBCD nanoparticles were used to study the cellular uptake in peritoneal macrophage cells as the amastigote cells reside within the phagolysosomes of macrophages. 4×10^5 macrophage cells/well in three batches were seeded with nanoparticles (0.5 mg/mL) and incubated in CO_2 incubator at 37 °C, for (A), 15 min; (B), 30 min; and (C), 60 min. Samples were withdrawn after these time intervals and observed in FITC channel under fluorescence microscope (magnification 60×, scale bar 10 μm). The prepared nanoparticles showed considerable increase in cellular internalization within 1 h of incubation when compared with 15 min.

1980). Thus, it is essential to investigate antileishmanial activity on amastigote forms. Piperolactam A showed promising antileishmanial activity on amstigote forms of wild-type as well as drug resistant strains of *L. donovani*.

5. Conclusions

In the present study, PL was isolated after bio-activity guided fractionation of crude root extract of *P. betle*. PL, representative of aristolactam alkaloids, exhibited strong antileishmanial activities against wild-type and drug resistant strains of *L. donovani*. The aqueous solubility of PL was enhanced after complexing with cyclodextrin which resulted in enhancement of selectivity and lowering of cellular toxicity. The crysllaine to amorphous conversion of PL in PL-HPBCD complex and complete incorporation of PL in cyclodextrin carrier was ascertained. Our developed stable (zeta potential of −28.6) nano-sphere (180 nm) showed considerable cellular internalization within 1 h of incubation. This research work can serve as a compendium of the potent activity of aristolactam structure being developed in this field and thus provides a new direction for development of antileishmanial chemotherapy.

Conflict of interest

The authors have declared that no competing interest exists.

Acknowledgements

This work was supported by a grant from Indian Council of Medical Research (ICMR), New Delhi, India (Grant No.: AMR/48/2011-ECD-I). Dr. Subhasish Mondal was awarded Research Associateship from ICMR to carry out this research work. Mr. Plaban Bhattacharya was awarded Senior Research Fellowship from Council of Scientific and Industrial Research (CSIR), New Delhi, India (Grant No.: 09/028(0814)/2010-EMR-I) which is also gratefully acknowledged. We would like to thank Dr. Shyamol Roy, Scientist, Indian Institute of Chemical Biology, Kolkata, India for his aid in procuring *L. donovani* strains.

Appendix A. Supplementary data

Supplementary data associated with this article can be found, in the online version, at http://dx.doi.org/10.1016/j.actatropica.2016.02.017.

References

Ali, I., Khan, F.G., Suri, K.A., Gupta, B.D., Satti, N.K., Dutt, P., et al., 2010. In vitro antifungal activity of hydroxychavicol isolated from *Piper betle* L. Ann. Clin. Microbiol. Antimicrob. 9, 7.
Alvar, J., Velez, I.D., Bern, C., Herrero, M., Desjeux, P., Cano, J., et al., 2012. WHO leishmaniasis control team: leishmaniasis worldwide and global estimates of its incidence. PLoS One 7, e35671.
Baek, J.S., Cho, C.W., 2013. 2-Hydroxypropyl-β-cyclodextrin-modified SLN of paclitaxel for overcoming p-glycoprotein function in multidrug-resistant breast cancer cells. J. Pharm. Pharmacol. 65 (1), 72–78.
Bhattacharjee, S., Bhattacharjee, A., Majumder, S., Majumdar, S.B., Majumdar, S., 2012. Glycyrrhizic acid suppresses Cox-2 mediated anti-inflammatory responses during *Leishmania donovani* infection. J. Antimicrob. Chemother. 67 (8), 1905–1914.
Bhattacharya, P., Saha, A., 2013. Evaluation of reversible contraceptive potential of *Cordia dichotoma* leaves extract. Rev. Bras. Farmacogn. 23 (2), 342–350.
Bhattacharya, P., Ghosh, M., Chatterjee, A., Bangal, S., Saha, A., 2014. Development of a validated stability-indicating high-performance thin-layer chromatographic method for the quantification of levetiracetam. J. Planar Chromatogr. 27 (2), 132–139.
Biyani, N., Singh, A.K., Mandal, S., Chawla, B., Madhubala, R., 2011. Differential expression of proteins in antimony-susceptible and resistant isolates of *Leishmania donovani*. Mol. Biochem. Parasitol. 179 (2), 91–99.
Carrizosa, M.J., Koskinen, W.C., Hermosin, M.C., 2004. Interactions of acidic herbicides bentazon and dicamba with organoclays. Soil Sci. Soc. Am J. 68 (6), 1863–1866.
Chakraborty, B., Biswas, S., Mondal, S., Bera, T., 2010. Stage specific developmental changes in the mitochondrial and surface membrane associated redox system of *Leishmania donovani* promastigote and amastigote. Biochemistry (Moscow) 75 (4), 494–504.
Chappuis, F., Sundar, S., Hailu, A., Ghalib, H., Rijal, S., Peeling, R.W., et al., 2007. Visceral leishmaniasis: what are the needs for diagnosis, treatment and control? Nat. Rev. Microbiol. 5 (11), 873–882.
Chen, S.T., Dou, J., Temple, R., Agarwal, R., Wu, K., Walker, S., 2008. New therapies from old medicines. Nat. Biotechnol. 26, 1077–1083.
Correa, J.E., Rios, C.H., Del, R.C.A., Romero, L.I., Ortega-Barria, E., Coley, P.D., et al., 2006. Minor alkaloids from *Guatteria dumetorum* with antileishmanial activity. Planta Med. 72 (3), 270–272.
Croft, S.L., Sundar, S., Fairlamb, A.H., 2006. Drug resistance in leishmaniasis. Clin. Microbiol. Rev. 19 (1), 111–126.
Debrabant, A., Joshi, M.B., Pimenta, P.F., Dwyer, D.M., 2004. Generation of *Leishmania donovani* axenic amastigotes: their growth and biological characteristics. Int. J. Parasitol. 34 (2), 205–217.
Demicheli, C., Ochoa, R., Silva, D.J.B., Falcao, C.A., Rossi-Bergmann, B., Melo, D.A.L., et al., 2004. Oral delivery of meglumine antimonite-beta-cyclodextrin complex for treatment of leishmaniasis. Antimicrob. Agents Chemother. 48 (1), 100–103.
Desai, S.J., Prabhu, B.R., Mulchandani, N.B., 1988. Aristolactams and 4,5-dioxoaporphines from *Piper longum*. Phytochemistry 27 (5), 1511–1515.
Dinan, L., Harmatha, J., Lafont, R., 2001. Chromatographic procedures for the isolation of plant steroids. J. Chromatogr. A 935 (1–2), 105–123.
Faraut-Gambarelli, F., Piarroux, R., Deniau, M., Giusiano, B., Marty, P., Michel, G., et al., 1997. In vitro and *in vivo* resistance of *Leishmania infantum* to meglumine antimoniate: a study of 37 strains collected from patients with visceral leishmaniasis. Antimicrob. Agents Chemother. 41 (4), 827–830.

Gradoni, L., Soteriadou, K., Louzir, H., Dakkak, A., Toz, S.O., Jaffe, C., et al., 2008. Drug regimens for visceral leishmaniasis in Mediterranean countries. Trop. Med. Int. Health 13 (10), 1272–1276.
Harborne, J.B., 1998. Phytochemical Methods: A Guide to Modern Techniques of Plant Analysis. Springer, London.
Huber, W., Koella, J.C., 1993. A comparision of the methods of estimating EC_{50} in studies of drug resistance of malaria parasites. Acta Trop. 55 (4), 257–261.
Iovannisci, D.M., Ullman, B., 1983. High efficiency plating method for *Leishmania* promastigotes in semi-defined or completely-defined media. J. Parasitol. 69 (4), 633–636.
Jackson, J.E., Tally, J.D., Ellis, W.Y., Mebrahtu, Y.B., Lawyer, P.G., Were, J.B., et al., 1990. Quantitative *in vitro* drug potency and drug susceptibility evaluation of *Leishmania* sp. from patients unresponsive to pentavalent antimony therapy. Am. J. Trop. Med. Hyg. 43 (5), 464–480.
Jhingran, A., Chawla, B., Saxena, S., Barett, M.P., Madhubala, R., 2009. Paromomycin: uptake and resistance in *Leishmania donovani*. Mol. Biochem. Parasitol. 164 (2), 111–117.
Kar, K., Mukherji, K., Naskar, K., Bhattacharya, A., Ghosh, D.K., 1990. *Leishmania donovani*: a chemically defined medium suitable for cultivation and cloning of promastigotes and transformation of amastigotes to promastigotes. J. Protozool. 37 (4), 277–279.
Lee, S.L., Dou, J., Agarwal, R., Temple, R., Beitz, J., Wu, C., et al., 2015. Evolution of traditional medicines to botanical drugs. Science 347, S32–S34.
Levrier, C., Balastrier, M., Beattie, K.D., Carroll, A.R., Martin, F., Choomuenwai, V., et al., 2013. Pyridocoumarin, aristolactam and aporphine alkaloids from the Australian rainforest plant *Goniothalamus australis*. Phytochemistry 86, 121–126.
Lin, C.F., Hwang, T.L., Chien, C.C., Tu, H.Y., Lay, H.L., 2013. A new hydroxychavicol dimer from the roots of *Piper betle*. Molecules 18 (3), 2563–2570.
Lira, R., Sundar, S., Makharia, A., Kenney, R., Gam, A., Saraiya, E., et al., 1999. Evidence that the high incidence of treatment failures in Indian kala-azar is due to the emergence of antimony-resistant strains of *Leishmania donovani*. J. Infect. Dis. 180 (2), 564–567.
Lo, W.L., Chang, F.R., Wu, Y.C., 2000. Alkaloids from the leaves of *Fissistigma glaucescens*. J. Chin. Chem Soc. 47 (6), 1251–1256.
Marques, A.M., Velozo, L.S., Moreira, D.D.L., Guimaraes, E.F., Kaplan, M.A., 2011. Aristolactams from roots of *Ottonia anisum* (Piperaceae). Nat. Prod. Commun. 6 (7), 939–942.
Mattock, N.M., Peters, W., 1975. The experimental chemotherapy of leishmaniasis. II. The activity in tissue culture of some antiparasitic and antimicrobial compounds in clinical use. Ann. Trop. Med. Parasitol. 69 (3), 359–371.
Memisoglu, E., Bochot, A., Ozalp, M., Sen, M., Duchene, D., Hincal, A.A., 2003. Direct formation of nanospheres from amphiphilic beta-cyclodextrin inclusion complexes. Pharm. Res. 20 (1), 117–125.
Miguel, D.C., Yokoyama-Yasunaka, J.K., Andreoli, W.K., Mortara, R.A., Uliana, S.R., 2007. Tamoxifen is effective against *Leishmania* and induces a rapid alkalinization of parasitophorus vacuoles harbouring *Leishmania* (*Leishmania*) *amazonensis* amastigotes. J. Antimicrob. Chemother. 60 (3), 526–534.
Misra, P., Kumar, A., Khare, P., Gupta, S., Kumar, N., Dube, A., 2009. Pro-apoptotic effect of the landrace Bangla Mahoba of *Piper betle* on *Leishmania donovani* may be due to the high content of eugenol. J. Med. Microbiol. 58 (8), 1058–1066.
Mondal, S., Roy, P., Das, S., Halder, A., Mukherjee, A., Bera, T., 2013. In Vitro susceptibilities of wild and drug resistant *Leishmania donovani* amastigote stages to andrographolide nanoparticle: role of vitamin E derivative TPGS for nanoparticle efficacy. PLoS One 8, e81492.
Mondal, S., Roy, J.J., Bera, T., 2014a. Characterization of mitochondrial bioenergetic functions between two forms of *Leishmania donovani*—a comparative analysis. J. Bioenerg. Biomembr. 46, 395–402.
Mondal, S., Roy, J.J., Bera, T., 2014b. Generation of adenosine tri-phosphate in *Leishmania donovani* amastigote forms. Acta Parasitol. 59 (1), 11–16.
Montenegro, H., Gutierrez, M., Romero, L.I., Ortega-Barria, E., Capson, T.L., Rios, L.C., 2003. Aporphine alkaloids from *Guatteria* spp: with leishmanicidal activity. Planta Med. 69 (7), 677–679.
Mookerjee, B.J., Mookerjee, A., Banerjee, R., Saha, M., Singh, S., Naskar, K., et al., 2008. Inhibition of ABC transporters abolishes antimony resistance in *Leishmania* infection. Antimicrob. Agents Chemother. 52 (3), 1080–1093.
Newman, D.J., Cragg, G.M., 2012. Natural products as sources of new drugs over the 30 years from 1981 to 2010. J. Nat. Prod. 75 (3), 311–335.
Nwaka, S., Hudson, A., 2006. Innovative lead discovery strategies for tropical diseases. Nat. Rev. Drug Discov. 5 (11), 941–955.
Odalo, J.O., Joseph, C.C., Nkunya, M.H., Sattler, I., Lange, C., Friedrich, G., et al., 2010. Aristolactams, 1-(2-C-methyl-beta-D-ribofuranosyl)-uracil and other bioactive constituents of *Toussaintia orientalis*. Nat. Prod. Commun. 5 (2), 253–258.
Peine, K.J., Gupta, G., Brackman, D.J., Papenfuss, T.L., Ainslie, K.M., Satoskar, A.R., et al., 2014. et al. Liposomal resiquimod for the treatment of *Leishmania donovani* infection. J. Antimicrob Chemother. 69 (1), 168–175.
Perez-Victoria, F.J., Castanys, S., Gamarro, F., 2003. *Leishmania donovani* resistance to miltefosine involves a defective inward translocation of the drug. Antimicrob. Agents Chemother. 47 (8), 2397–2403.
Peters, W., Trotter, E.R., Robinson, B.L., 1980. The experimental chemotherapy of leishmaniasis, VII. Drug responses of *L. major* and *L. mexicana* amazonensis, with an analysis of promising chemical leads to new antileishmanial agents. Ann. Trop. Med. Parasitol. 74 (3), 321–335.
Pucadyil, T.J., Tewary, P., Madhubala, R., Chattopadhyay, A., 2004. Cholesterol is required for *Leishmania donovani* infection: implications in leishmaniasis. Mol. Biochem. Parasitol. 133 (2), 145–152.
Rasoanaivo, P., Wright, C.W., Willcox, M.L., Gilbert, B., 2011. Whole plant extracts versus single compounds for the treatment of malaria: synergy and positive interactions. Malar. J. 10 (Suppl. 1), S4.
Reithinger, R., Dujardin, J.C., Louzir, H., Pirmez, C., Alexander, B., Brooker, S., 2007. Cutaneous leishmaniasis. Lancet Infect. Dis. 7 (9), 581–596.
Rojas, R., Valderrama, L., Valderrama, M., Varona, M.X., Ouellette, M., Saravia, N.G., 2006. Resistance to antimony and treatment failure in human *Leishmania* (Viannia) infection. J. Infect. Dis. 193 (10), 1375–1383.
Roy, P., Das, S., Bera, T., Mondol, S., Mukherjee, A., 2010. Andrographolide nanoparticles in leishmaniasis: characterization and *in vitro* evaluations. Int. J. Nanomed. 5, 1113–1121.
Sarkar, A., Sen, R., Saha, P., Ganguly, S., Mandal, G., Chatterjee, M., 2008. An ethanolic extract of leaves of *Piper betle* (Paan) Linn mediates its antileishmanial activity via apoptosis. Parasitol. Res. 102 (6), 1249–1255.
Sasidharan, S., Chen, Y., Saravanan, D., Sundram, K.M., Yoga, L.L., 2011. Extraction, isolation and characterization of bioactive compounds from plants extracts. Afr. J. Tradit. Complement. Altern. Med. 8 (1), 1–10.
Silva, F.M.A.D., Koolen, H.H.F., Lima, J.P.S.D., Santos, D.M.F., Jardim, I.S., Souza, A.D.L.D., et al., 2012. Leishmanicidal activities of fractions rich in aporphine alkaloids from Amazonian *Unonopsis* species. Rev. Bras. Farmacogn. 22 (6), 1368–1371.
Singh, P.S., Kumar, M., 2014. Current treatment of visceral leishmaniasis (Kala-azar): an overview. Int. J. Res. Med. Sci. 2 (3), 810–817.
Siqueira-Neto, J.L., Song, O., Oh, H., Sohn, J., Yang, G., Nam, J., et al., 2010. Antileishmanial high-throughput drug screening reveals drug candidates with new scaffolds. PLoS Negl. Trop. Dis. 4 (5), e675.
Stella, V.J., He, Q., 2008. Cyclodextrins. Toxicol. Pathol. 36 (1), 30–42.
Sundar, S., More, D.K., Singh, M.K., Singh, V.P., Sharma, S., Makharia, A., 2000. Failure of pentavalent antimony in visceral leishmaniasis in India: report from the center of the Indian epidemic. Clin. Infect. Dis. 31 (4), 1104–1107.
Teixeira, M.C., Jesus, D.S.R., Sampaio, R.B., Pontes-de-Carvalho, L., dos-Santos, W.L., 2002. A simple and reproducible method to obtain large numbers of axenic amastigotes of different *Leishmania* species. Parasitol. Res. 88 (11), 963–968.
Thakur, C.P., Pandey, A.K., Sinha, G.P., Roy, S., Behbehani, K., Olliaro, P., 1996. Comparison of three treatment regimens with liposomal amphotericin B (AmBisome) for visceral leishmaniasis in India: a randomized Dose-finding study. Trans. R. Soc. Trop. Med. Hyg. 90 (3), 319–322.
Waechter, A.I., Cave, A., Hocquemiller, R., Bories, C., Munoz, V., Fournet, A., 1999. Antiprotozoal activities of aporphine alkaloids isolated from *Unonopsis buchtienii* (Annonaceae). Phytother. Res. 13 (2), 175–177.
Yang, D.L., Mei, W.L., Wang, H., Dai, H.F., 2010. Antimicrobial alkaloids from the tubers of *Stephania succifera*. Z. Naturforsch. Sect. B 65, 757–761.